Received: 15 March 2021 | Revised: 28 August 2021 | Accepted: 31 August 2021

DOI: 10.1111/jbi.14267

Journal of Biogeography WILEY

RESEARCH ARTICLE

Genomic inferences in a thermophilous grasshopper provide insights into the biogeographic connections between northern African and southern European arid-dwelling faunas

Joaquín Ortego[1] | María José González-Serna[2] | Víctor Noguerales[3,4] | Pedro J. Cordero[2,5]

[1]Department of Integrative Ecology, Estación Biológica de Doñana (EBD-CSIC), Seville, Spain

[2]Grupo de Investigación de la Biodiversidad Genética y Cultural, Instituto de Investigación en Recursos Cinegéticos (IREC, CSIC-UCLM-JCCM), Ciudad Real, Spain

[3]Department of Biological Sciences, University of Cyprus, Nicosia, Cyprus

[4]Instituto de Productos Naturales y Agrobiología (IPNA-CSIC), La Laguna, Spain

[5]Escuela Técnica Superior de Ingenieros Agrónomos (ETSIA) de Ciudad Real, Universidad de Castilla-La Mancha (UCLM), Ciudad Real, Spain

Correspondence
Joaquín Ortego, Department of Integrative Ecology, Estación Biológica de Doñana, EBD-CSIC, Avda. Américo Vespucio 26, E-41092 Seville, Spain.
Email: joaquin.ortego@csic.es

Funding information
European Social Fund, Grant/Award Number: CGL2011-25053, CGL2014-54671-P, CGL2016-80742-R and CGL2017-83433-P; Spanish Ministry of Economy, Industry and Competitiveness

Handling Editor: Greer Dolby

Abstract

Aim: Although thermophilous and arid-dwelling relict biotas constitute a singular component of European biodiversity of high conservation value, we still largely ignore their biogeographic history. In this study, we investigate the geographical diversification of the Maghrebian-Levantine crested grasshopper and its colonization of semiarid habitats of southeastern Iberia to gain insights into the historical processes underlying the biogeographic connections between northern African and southern European arid-dwelling faunas.

Location: Mediterranean region.

Taxon: Crested grasshoppers *Dericorys millierei* and *Dericorys carthagonovae* (Orthoptera: Dericorythidae).

Methods: We used genomic data (ddRAD-seq) to quantify the genetic structure of populations, infer the phylogenetic relationships among them, estimate divergence times, and elucidate the demographic processes accompanying the colonization of southeastern Iberia. Genomic-based inferences were interpreted in the light of eustatic sea-level reconstructions and species' range dynamics derived from palaeodistribution modelling at fine temporal resolution.

Results: Clustering analyses showed a strong genetic structure and phylogenomic inference revealed that Iberian populations are nested within a Maghrebian clade. Molecular dating analyses indicated that all lineages diverged during the Pleistocene (<1.6 Ma), with point estimates coinciding with glacial periods and the accompanying sea level drops. According to palaeodistribution modelling, the species experienced severe range contractions during the coldest stages of the Pleistocene.

Main conclusions: Our results indicate that the colonization of the Iberian Peninsula likely took place during the marked sea level drops characterizing the high-amplitude climatic oscillations of the late Quaternary (<0.5 Ma), which considerably reduced overseas distances between northern African and southern European landmasses and

might have eased transmarine exchanges of terrestrial faunas. These findings emphasize the high relevance of the Maghreb region as a source of European thermophilous biotas and corroborate post-Messinian biogeographic connections between the two continents despite the barrier effect of the Mediterranean Sea.

KEYWORDS
Dericorys carthagonovae, *Dericorys millierei*, genetic fragmentation, palaeodistribution modelling, phylogenomic inference, Pleistocene glacial cycles, transmarine dispersal

1 | INTRODUCTION

Narrowly distributed thermophilous, arid-adapted, and steppe-dwelling biotas constitute a singular component of European biodiversity, often including relict species that are the only living representatives in the continent at different taxonomic ranks (Husemann et al., 2014; Kajtoch et al., 2016; Ribera & Blasco-Zumeta, 1998). In some instances, these taxa show remarkable genetic distinctiveness (i.e., vicariant lineages, subspecies or even species) with respect to core distributions in Central Asia or North Africa, representing a unique evolutionary legacy of high conservation value (Husemann et al., 2014; Kajtoch et al., 2016; Kirschner et al., 2020). Despite recent advances, the temporal and geographic origin of thermophilous and arid-dwelling European species is not yet well understood, which in part might be due to the extraordinarily dynamic geological history of the region and the difficulty to distinguish among alternative biogeographical scenarios (Noguerales et al., 2021; Ribera & Blasco-Zumeta, 1998). Miocene-Pliocene movements of African and Asian continental plates led to the permanent closing of the eastern end of the current Mediterranean Sea (c. 23–14 Ma) and the temporal closure of the Mediterranean-Atlantic seaways during the Messinian Salinity Crisis (c. 5.96–5.33 Ma; Bialik et al., 2019; Meulenkamp & Sissingh, 2003), which contributed to faunal and floral exchanges between Africa, Europe and Asia (e.g., Faille et al., 2014; Manafzadeh et al., 2014; Sanmartín, 2003). However, several studies have also found post-Messinian colonization and considerable genetic cohesiveness between thermophilous and arid-adapted biotas of Europe and those from North Africa (Husemann et al., 2014) and Central Asia steppes (Kirschner et al., 2020), indicating that their current disjunct distributions are most likely a consequence of range expansion-fragmentation dynamics linked to Pleistocene climatic oscillations (e.g., Habel et al., 2010; Noguerales et al., 2021). In some other cases, the role of human-mediated dispersal or historical introductions in the distribution of some thermophilous organisms in southern Europe cannot be discarded (Husemann et al., 2014).

A paradigmatic case of European thermophilous relict biotas is exemplified in the biogeographic connections between the semideserts characterizing southeastern Iberia and arid regions from North Africa and the Middle East (Le Driant & Carlon, 2020). Although it has been long speculated about the anthropic origin of semidesert areas from the Iberian Peninsula, mounting biogeographical evidence points to the persistence of at least some naturally deforested enclaves through the Pleistocene linked to arid spots with gypsum and saline soils (Ribera & Blasco-Zumeta, 1998). This end is supported by the presence in Iberian semiarid habitats of multiple relict species shared with Maghrebian, Saharo-Arabian and Irano-Turanian regions and whose distributions in the region likely predate anthropic deforestation (Le Driant & Carlon, 2020; Ribera & Blasco-Zumeta, 1998). In the specific case of southeastern Iberia, these taxa include strictly thermophilous, xerophytic and deserticolous plants (Cabello et al., 2003; Le Driant & Carlon, 2020; Sánchez-Gómez et al., 2013), arthropods (Bolívar, 1897; Pascual & Aguirre, 1996), and vertebrates (Barrientos et al., 2009; Graciá, Giménez, et al., 2013). Two main hypotheses have been postulated to explain the distribution of these faunas and floras in arid habitats from southern Europe: (i) long-term persistence of relictual biotas that presented a much wider distribution during the Miocene-Pliocene and expanded during the partial desiccation of the Mediterranean Sea in the Messinian Salinity Crisis; (ii) Quaternary colonization linked to recurrent expansions-contractions of suitable habitats and alterations in the proximity between northern African and southern European landmasses fuelled by Pleistocene climatic and eustatic sea-level oscillations (Graciá, Giménez, et al., 2013; Ribera & Blasco-Zumeta, 1998; Sanmartín, 2003).

In the present study, we integrate genome-wide nuclear data with eustatic sea-level and palaeodistribution reconstructions at fine temporal resolutions to shed light on the historical processes underlying the geographical diversification and colonization history of thermophilous faunas shared between northern Africa and southern European arid and semiarid habitats. Specifically, we focus on two closely related taxa of thermophilous crested grasshoppers: *Dericorys millierei* Bonnet & Finot, 1884 and *Dericorys carthagonovae* Bolívar, 1897 (Orthoptera: Dericorythidae). *Dericorys millierei* presents a wide trans-Mediterranean distribution, with a continuous range across the Maghrebian region (Morocco, Algeria, Tunisia and Libya) and disjunct populations in a small area of the Middle East (Israel, Palestine and Jordan; Figure 1). In contrast, *D. carthagonovae* is a narrowly distributed taxon exclusively present in semiarid areas of southeastern Iberia (Figure 1), where it forms highly fragmented populations linked to vegetation growing in salty and brackish grounds (Verdú et al., 2011). The narrow distribution of *D. carthagonovae* and the continuous decline of its populations due to extensive destruction of suitable habitats for agricultural and urban

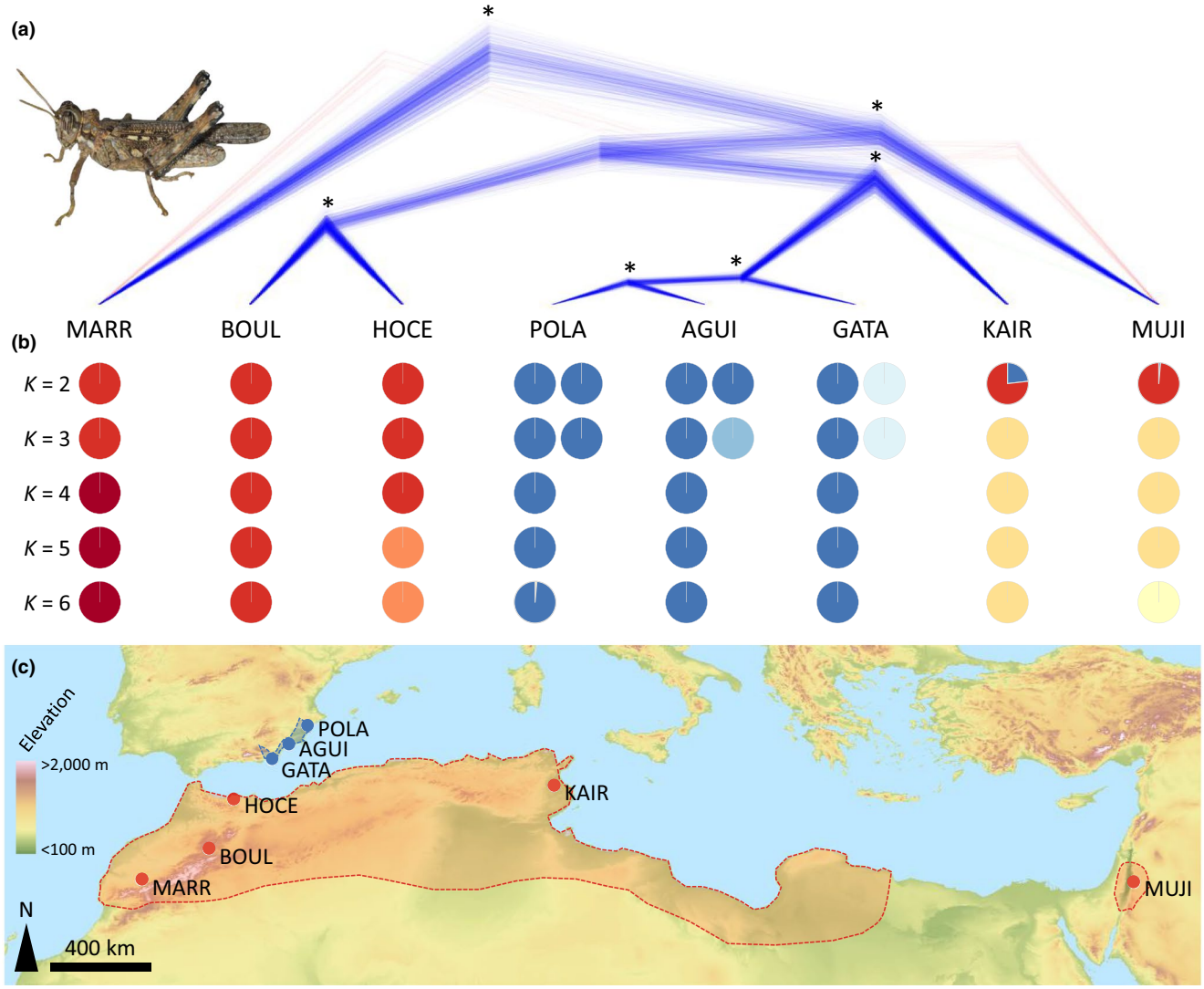

FIGURE 1 (a) Phylogenetic relationships among populations as inferred by SNAPP (3115 SNPs), (b) genetic assignments of populations based on the Bayesian method implemented in the program STRUCTURE, and (c) map showing the approximate distribution ranges (shaded areas) and geographical location of sampling localities (dots) for *Dericorys carthagonovae* (in blue) and *D. millierei* (in red) across the Mediterranean region. SNAPP tree shows the first (blue) and second (red) most supported topologies and Bayesian posterior probabilities are indicated on the nodes (* = 1). STRUCTURE analyses were run for all populations (10,000 SNPs) and independently for populations of *D. carthagonovae* (10,000 SNPs, pie charts on right). Map in EPSG:4326 (WGS84) projection and population codes as described in Table 1. Inset image shows a male of *D. carthagonovae* (picture by Francisco Rodríguez)

development has led to the inclusion of the species in the IUCN Red List of Threatened Species with the category "Endangered" (Hochkirch et al., 2016; Verdú et al., 2011). Although *D. carthagonovae* is a singular species of high conservation concern, being the only representative of the genus in Europe, its taxonomic status is controversial. The species was first recorded in southeastern Iberia by Bolívar (1897), who described it as a "variety" of *D. millierei*. The taxon was subsequently upgraded to species rank without any justification in the synonymic catalogue by Kirby (1910), a status that has been accepted and used since then (Cigliano et al., 2021).

We first tested the contrasting hypotheses that the current ranges of the two taxa are a consequence of Miocene persistence followed by vicariance events after the Messinian Salinity Crisis (>5.3 Ma; e.g., Martínez-Solano et al., 2004; Ribera & Blasco-Zumeta, 1998) or if, instead, their distributions resulted from more recent pulses of range expansion and fragmentation linked to Pleistocene climatic oscillations (<2.6 Ma; e.g., Fritz et al., 2009; Noguerales et al., 2021; Stöck et al., 2008). Second, we tested the hypothesis that the colonization of the Iberian Peninsula took place coinciding with sea-level lowering during glacial periods, which might have increased the chance of successful passive dispersal by rafting and stepping-stone dispersal (Houle, 1998; Husemann et al., 2014). Finally, we quantified spatial patterns of genetic structure and tested whether the timing of genetic subdivision among populations of the red-listed *D. carthagonovae* is compatible with human-induced habitat fragmentation or, alternatively, a consequence of ancient processes predating the impacts of anthropogenic activities (González-Serna et al., 2019; Zellmer & Knowles, 2009).

2 | MATERIALS AND METHODS

2.1 | Population sampling

We sampled populations of *Dericorys carthagonovae* in the Iberian Peninsula (Spain, $n = 3$ populations) and *Dericorys millierei* in the Maghreb (Morocco and Tunisia, $n = 4$ populations) and the Middle East (Jordan, $n = 1$ population; Table 1; Figure 1). We used occurrence records available in the literature to design sampling and collect specimens from populations covering the entire distribution ranges of the two taxa (Figure 1). We obtained genomic data for 35 individuals of the two taxa, with an average of four individuals per locality (range = 2–5; Table 1). Samples of *Dericorys lobata lobata* (Brullé, 1840) (10 individuals), *Dericorys lobata luteipes* Uvarov, 1938 (four individuals), and *Dericorys minutus* Chopard, 1954 (one individual) collected from the Canary Islands (Table 1) were used as outgroups in phylogenomic analyses. We registered spatial coordinates using a Global Positioning System (GPS) and preserved whole specimens at −20°C in 1500 μl ethanol 96% until needed for genomic analyses. Further details on sampling locations are provided in Table 1.

2.2 | Genomic library preparation and genomic data processing

We used NucleoSpin Tissue (Macherey-Nagel) kits to extract and purify DNA from a hind leg of each individual. We processed genomic DNA into one genomic library using the double-digestion restriction-site associated DNA sequencing procedure (ddRAD-seq) described in Peterson et al. (2012). In brief, we digested DNA with the restriction enzymes MseI and EcoRI (New England Biolabs) and ligated Illumina adaptors including unique 7-bp barcodes to the digested fragments of each individual. We pooled ligation products and size-selected them between 475 and 580 bp with a Pippin Prep machine (Sage Science). We amplified the fragments by PCR with 12 cycles using the iProofTM High-Fidelity DNA Polymerase (BIO-RAD) and sequenced the library in a single-read 151-bp lane on an Illumina HiSeq2500 platform at The Centre for Applied Genomics (Toronto, ON, Canada). Raw sequences were demultiplexed and preprocessed using STACKS v. 1.35 (Catchen et al., 2011, 2013) and assembled using PYRAD v. 3.0.66 (Eaton, 2014; e.g., Ortego et al., 2018). Methods S1 provides all details on sequence assembling and data filtering.

2.3 | Genetic structure analyses

We analysed population genetic structure and admixture using STRUCTURE v. 2.3.3 (Pritchard et al., 2000). We ran two independent STRUCTURE analyses, one including all populations of *D. carthagonovae* and *D. millierei* and another focused on the three populations of *D. carthagonovae*. In both cases, we ran STRUCTURE using a random subset of 10,000 SNPs, with 200,000 MCMC cycles after a burn-in step

TABLE 1 Locality, country, code, latitude, longitude, number of genotyped individuals (n), and genetic diversity statistics (π, nucleotide diversity; Hd, haplotype – gene – diversity; θ, population size parameter) for each sampled species and population

Species	Locality	Country	Code	Latitude	Longitude	n	π	Hd	θ
Dericorys carthagonovae	Santa Pola	Spain	POLA	38.205615	−0.613583	5	0.0008	0.0552	0.0097
Dericorys carthagonovae	Águilas	Spain	AGUI	37.432109	−1.524628	5	0.0006	0.0426	0.0052
Dericorys carthagonovae	Cabo de Gata	Spain	GATA	36.780914	−2.231885	4	0.0003	0.0252	0.0026
Dericorys millierei	Marrakesh	Morocco	MARR	31.649482	−7.926335	5	0.0012	0.0877	0.0092
Dericorys millierei	Boulaajoul	Morocco	BOUL	32.896938	−4.970910	4	0.0031	0.1396	0.0146
Dericorys millierei	Al Hoceima	Morocco	HOCE	35.193799	−3.864230	5	0.0020	0.0934	0.0125
Dericorys millierei	Kairouan	Tunisia	KAIR	35.682503	10.224624	5	0.0086	0.3440	0.0554
Dericorys millierei	Wadi Al Mujib	Jordan	MUJI	31.446110	35.796170	2	0.0036	0.1751	0.0226
Dericorys lobata lobata	Lanzarote	Spain	LANZ	28.862974	−13.855643	10	—	—	—
Dericorys lobata luteipes	Fuerteventura	Spain	FUER	28.390268	−13.861184	4	—	—	—
Dericorys minutus	Gran Canaria	Spain	GCAN	28.147701	−15.694875	1	—	—	—

of 100,000 iterations, and assuming correlated allele frequencies and admixture. We conducted 15 independent runs for each value of *K*-clusters, where *K* ranged from 1 to *n* + 1 for each dataset of *n* sampled populations. We retained the ten runs having the highest likelihood for each value of *K* and evaluated the number of genetic clusters that best describes our data according to log probabilities of the data (LnPr(X|*K*; Pritchard et al., 2000) and the Δ*K* method (Evanno et al., 2005), as implemented in STRUCTURE HARVESTER (Earl & vonHoldt, 2012). We used CLUMPP v. 1.1.2 and the Greedy algorithm to align multiple runs of STRUCTURE for the same *K* value (Jakobsson & Rosenberg, 2007) and DISTRUCT v. 1.1 (Rosenberg, 2004) to visualize as bar plots the individual's probabilities of population membership. Complementary to Bayesian clustering analyses, we performed a principal component analysis (PCA) as implemented in the R v. 4.0.3 (R Core Team, 2021) package 'adegenet' (Jombart, 2008). Before running the PCA, we replaced missing data by the mean frequency of the corresponding allele estimated across all samples (Jombart, 2008).

2.4 | Phylogenomic inference

First, we reconstructed the phylogenetic relationships among populations of *D. carthagonovae* and *D. millierei* using three independent analytical approaches: SNAPP v. 1.3 (Bryant et al., 2012), BPP v. 4.1 (Flouri et al., 2018), and SVDQUARTETS (Chifman & Kubatko, 2014). Second, we used PHYLONETWORKS (Solís-Lemus et al., 2017) and TREEMIX v. 1.12 (Pickrell & Pritchard, 2012) to assess the potential presence and direction of gene flow between non-sister lineages that might result in conflicting phylogenetic relationships and distort tree topology. Methods S2 provides all details on the specific settings used to perform phylogenomic analyses.

2.5 | Estimation of divergence time

We used analysis A00 in BPP to estimate the posterior distribution of divergence times (τ; Flouri et al., 2018; Rannala & Yang, 2003). We ran the analyses using the same dataset and settings considered for tree inference analyses in BPP described in Methods S2. We estimated divergence times using the equation $\tau = 2\mu t$, where τ is the divergence in substitutions per site estimated by BPP, μ is the per site mutation rate per generation, and t is the absolute divergence time in years (Huang et al., 2020; Walsh, 2001). We considered the mutation rate per site per generation of 2.8×10^{-9} estimated for *Drosophila melanogaster* (Keightley et al., 2014; e.g., Tonzo et al., 2020). Finally, we used paleo sea-level reconstructions to test whether the colonization of the Iberian Peninsula took place coinciding with the lowering of sea levels during the coldest stages of the Pleistocene (Miller et al., 2011). Specifically, we considered the sea-levels estimated by Miller et al. (2011) at each time period contained within the high posterior density (HPD) intervals of divergence times and used one-sample *t* tests to determine whether they significantly differ from sea level at present time (i.e., 0 m a.s.l.).

2.6 | Demographic analyses

We used the composite-likelihood simulation-based approach implemented in FASTSIMCOAL2 (Excoffier et al., 2013) to estimate the timing of colonization of southeastern Iberia, which is expected to coincide with a demographic bottleneck (i.e., a founder event) predating in situ geographical diversification (e.g., Graciá, Giménez, et al., 2013). We considered that northernmost populations POLA and AGUI share a most recent common ancestor, as supported by phylogenomic analyses (see Section 3) and the comparatively much lower composite likelihood of pilot runs for alternative topological relationships. We calculated a folded joint site frequency spectrum (SFS) considering a single SNP per locus to avoid the effects of linkage disequilibrium. To remove all missing data for the calculation of the joint SFS, minimize errors with allele frequency estimates and maximize the number of variable SNPs retained, each population group was downsampled to *n*-1 of individuals (i.e., four individuals for POLA and AGUI and three individuals for GATA; Table 1) using the *easySFS.py* script (I. Overcast, https://github.com/isaacovercast/easySFS). The SFS contained 5637 variable SNPs. Because invariable sites were excluded from likelihood calculations ('removeZeroSFS' option in FASTSIMCOAL2), we fixed the effective population size for one of the demes (POLA) to enable the estimation of other parameters (Excoffier et al., 2013). The effective population size fixed in the model was calculated from the level of nucleotide diversity (π) and estimates of mutation rate per site per generation (μ; 2.8×10^{-9}; Keightley et al., 2014). Nucleotide diversity (π) was estimated from polymorphic and non-polymorphic loci using DNASP v. 6.12.03 (Rozas et al., 2017). The model was run 100 replicated times considering 100,000–250,000 simulations for the calculation of the composite likelihood, 10–40 expectation-conditional maximization (ECM) cycles, and a stopping criterion of 0.001 (Excoffier et al., 2013). Point estimates for the different demographic parameters were selected from the replicate with the highest maximum composite likelihood. Finally, we calculated confidence intervals of parameter estimates from 100 parametric bootstrap replicates by simulating SFS from the maximum composite likelihood estimates and re-estimating parameters each time (Excoffier et al., 2013).

2.7 | Population genetic diversity

We calculated levels of haplotype (gene) diversity (Hd) and nucleotide diversity (π) of the different populations using DNASP and tested whether they differ between taxa (one-way ANOVAs) and are explained by geography (i.e., latitude and longitude; linear regressions). Additionally, we calculated contemporary population size parameters (θ) and their respective 95% high posterior density (HPD) intervals in SNAPP as detailed for phylogenomic analyses in Methods S2.

2.8 | Environmental niche modelling

We built an environmental niche model (ENM) to predict the geographic distribution of climatically suitable habitats for *D. millierei* and *D. carthagonovae* from the last glacial maximum (LGM, 22 ka) to present. To build the ENM, we used the maximum entropy algorithm implemented in MAXENT v.3.3.3 (Phillips et al., 2006; Phillips & Dudik, 2008) and the 19 bioclimatic variables from the CHELSA database (as described at http://chelsa-climate.org/bioclim/) interpolated to 30-arcsec resolution (Karger et al., 2017a, 2017b). To estimate environmental suitability from the LGM to present, we projected the ENM to bioclimatic conditions during the last 22,000 years at 100-year time intervals (i.e., from 1990 CE to the LGM). Bioclimatic layers at these temporal snapshots are based on a variant of the CHELSA v. 1.2 algorithm (Karger et al., 2017) on the TraCE-21 ka data (Liu et al., 2009) and are available at a high resolution (30-arcsec) from the CHELSA database (https://chelsa-climate.org/; Karger et al., 2017; Yannic et al., 2020). As several lines of evidence indicate that *D. millierei* and *D. carthagonovae* should be synonymized (see Section 4), we built a single ENM based on records available for the two currently recognized taxa. Further details on ENM are presented in Methods S3.

3 | RESULTS

3.1 | Genomic data

The average number of reads retained per individual after the different quality filtering steps was 2,021,895 (range = 886,652–3,682,528 reads; Figure S1). On average, this represented 84% (range = 75%–86%) of the total number of reads recovered for each individual (Figure S1). Final datasets obtained considering a clustering threshold of sequence similarity of 0.85 (W_{clust} = 0.85) and discarding loci that were not present in at least 50% individuals (*minCov* = 50%) contained 18,550 SNPs for the dataset including all populations of *D. carthagonovae* and *D. millierei*, and 36,483 SNPs for the dataset only including the three populations of *D. carthagonovae*.

3.2 | Genetic structure analyses

STRUCTURE analyses including populations of *D. carthagonovae* and *D. millierei* identified that the most likely number of clusters was $K = 2$ according to the ΔK criterion, but LnPr(X|K) steadily increased up to $K = 6$ (Figure S2a). For $K = 2$, the two genetic clusters separated populations of *D. carthagonovae* and *D. millierei* (Figure 1; Figure S3). Only the population from Tunisia (KAIR) was admixed, with c. 25% of probability of assignment to the genetic cluster mainly represented in the Iberian *D. carthagonovae* (Figure 1; Figure S3). Analyses for $K = 3$–6 sequentially split the different populations of *D. millierei* in different genetic clusters, which showed no signatures of genetic admixture among them (Figure 1; Figure S3). Analyses focused on the three populations of *D. carthagonovae* showed that LnPr(X|K) reached a plateau at $K = 3$ and ΔK peaked at the same K value (Figure S2b). In these analyses, $K = 2$ split the southernmost population GATA from POLA and AGUI (Figure 1; Figure S3). For $K = 3$, the three populations of *D. carthagonovae* were assigned to different genetic clusters that showed no admixture among them (Figure 1; Figure S3). Principal component analysis (PCA) separated *D. millierei* from *D. carthagonovae* along the PC1, whereas populations of *D. millierei* split along the PC2 in the three main genetic clusters (MARR, BOULHOCE, and KAIR-MUJI) identified by STRUCTURE analyses (Figure S4).

3.3 | Phylogenomic inference

Phylogenomic analyses revealed that *D. carthagonovae* is monophyletic and nested within *D. millierei*, which is a paraphyletic taxon (Figure 1; Figure S5). The population of *D. millierei* from Marrakech (MARR) was sister to the remaining populations, including those from the Iberian *D. carthagonovae*, which shared a most recent common ancestor with the Tunisian population (KAIR) of *D. millierei* (Figure 1; Figure S5). The only incongruence among the different analyses was the phylogenetic position of the population from Jordan (MUJI). BPP and SVDQUARTETS analyses supported that MUJI was sister to the subclade including *D. carthagonovae* (POLA, AGUI, and GATA) and the Tunisian population (KAIR) of *D. millierei* (Figure S5). However, SNAPP analyses supported that MUJI was sister to the clade including *D. carthagonovae* and the remaining populations of *D. millierei* (excluding MARR; Figure 1). Although this was the only topology contained in the 95% HPD tree set and all nodes were fully supported, the second most supported topology yielded by SNAPP was identical to that obtained by BPP and SVDQUARTETS (Figure 1). All nodes were also fully supported in BPP analyses (Figure S5). Phylogenetic inference using SVDQUARTETS was little affected by different schemes of data filtering and all SNP datasets yielded the same topology (Figure S5; e.g., Noguerales et al., 2018; Takahashi et al., 2014). However, the phylogenetic relationships among populations within the clade including *D. carthagonovae* (POLA, AGUI, and GATA) and the Tunisian (KAIR) and Jordanian (MUJI) populations of *D. millierei* were not always well resolved by SVDQUARTETS, particularly in those analyses based on matrices retaining a lower number of SNPs (i.e., *minCov* = 25% and 50%; Figure S5). PHYLONETWORKS and TREEMIX analyses showed that models considering a strictly bifurcating tree with no introgression edges (i.e., $m = 0$) are statistically indistinguishable (ΔAIC < 1.4) or more supported than models with one or more migration events, indicating no evidence for post-divergence gene flow between non-sister lineages (Table S1). PHYLONETWORKS and TREEMIX retrieved the same topology than BPP and SVDQUARTETS (Figure S6).

3.4 | Divergence time estimation

BPP analyses (A00 model) estimated that all populations diverged from a common ancestor during the early Pleistocene (c. 1.6 Ma;

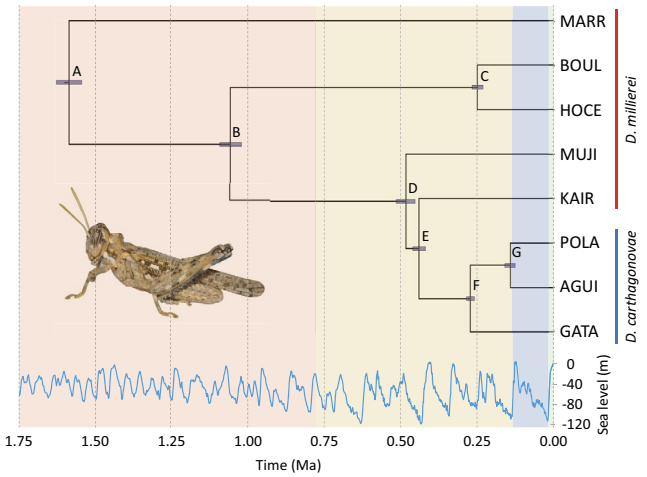

FIGURE 2 Phylogenetic tree and divergence times estimated using BPP for the analysed populations of *Dericorys carthagonovae* and *D. millierei* across the Mediterranean region. Bars on nodes indicate 95% highest posterior densities (HPD) of divergence times estimated considering a genomic mutation rate of 2.8×10^{-9} per site per generation and a one-year generation time. Background colours indicate geological divisions of the Quaternary (red: early Pleistocene; yellow: middle Pleistocene; blue: upper Pleistocene; green: Holocene). Sea level estimates based on Miller et al. (2011). Population codes as described in Table 1. Inset image shows a male of *D. carthagonovae* (picture by Francisco Rodríguez)

Calabrian age; Figure 2). All populations of the Maghrebian *D. millierei* split during the early and middle Pleistocene, starting with the divergence of MARR from the rest of the populations (c. 1.6 Ma; Calabrian age) and ending with the split of HOCE and BOUL (c. 0.25 Ma; Chibanian age; Figure 2). Finally, Iberian populations of *D. carthagonovae* diverged among them (c. 0.27–0.14 Ma) and from their sister lineage of *D. millierei* (KAIR; c. 0.44 Ma) during the middle Pleistocene (Chibanian age; Figure 2). The split of the different lineages took place during glacial periods, when sea levels were significantly below current shoreline (one-sample *t* tests, $t < -11.70$, $p < 0.001$ for all nodes; Figure S7). The colonization of the Iberian Peninsula was estimated to take place coinciding with the Mindel glaciation (Figure 2), when the sea level dropped to the minimum value of the entire Pleistocene (−123 m; Figure S7).

3.5 | Demographic analyses

FASTSIMCOAL2 analyses showed that the most recent common ancestor of southeastern Iberian populations experienced a demographic bottleneck during the Mindel glaciation, which resulted in a reduction of ancestral effective population sizes by c. 39% (Table 2; Figure 3). Remarkably, the point estimate for the timing of the demographic bottleneck (437 ka) is very similar to the stem age (440 ka) calculated in BPP for the divergence between Tunisian and the most recent common ancestor of southeastern Iberian populations (Figure 2). It must be noted, however, that there is considerable uncertainty around the estimation of parameters for more ancient demographic events (especially θ_{ANC} and T_{BOT}; Table 2), which can in part be explained by the very small samples sizes available for each population (4–5 individuals/population; Table 1). In situ geographical diversification of *D. carthagonovae* was estimated to take place during the last interglacial-glacial transition (Riss-Würm), with an initial split of GATA from the rest of the populations (c. 130 ka) followed shortly after by the divergence between POLA and AGUI (c. 124 ka; Table 2; Figure 3).

3.6 | Population genetic diversity

Levels of nucleotide diversity (π) and haplotype diversity (Hd), and estimates of the population size parameter (θ) did not significantly differ between *D. millierei* and *D. carthagonovae* (one-way ANOVAs, π: $F_{1,6} = 3.27$, $p = 0.121$; Hd: $F_{1,6} = 4.09$, $p = 0.090$; θ: $F_{1,6} = 2.25$, $p = 0.184$; Table 1; Figure 4). Estimates of genetic diversity were not correlated with latitude (π: $r = 0.21$, $F_{1,6} = 0.29$, $p = 0.611$; Hd: $r = 0.29$, $F_{1,6} = 0.54$, $p = 0.489$; θ: $r = 0.13$, $F_{1,6} = 0.11$, $p = 0.752$) nor longitude (π: $r = 0.43$, $F_{1,6} = 1.40$, $p = 0.282$; Hd: $r = 0.47$, $F_{1,6} = 1.75$, $p = 0.234$; θ: $r = 0.45$, $F_{1,6} = 1.50$, $p = 0.266$). Population of *D. millierei* from Tunisia (KAIR) stood out for its high levels of genetic diversity, which were significantly higher than those observed in the remaining study populations (one-sample *t* tests; π: $t = -14.34$,

TABLE 2 Parameters inferred from coalescent simulations with FASTSIMCOAL2 under a model of colonization of southeastern Iberia (i.e., hypothetically coinciding with a demographic bottleneck resulted from a founder event) followed by in situ geographical diversification of *Dericorys carthagonovae* (see Figure 3 for details)

Parameter	Point estimate	Lower bound	Upper bound
T_{BOT}	437,434	230,154	959,203
T_{DIV1}	130,165	129,963	166,359
T_{DIV2}	124,281	116,718	134,751
θ_{ANC}	297,960	55,935	466,391
θ_{BOT}	119,098	57,953	132,580
$\theta_{POLA\text{-}AGUI}$	6991	10,397	42,264
θ_{POLA}	140,746	–	–
θ_{AGUI}	57,150	52,521	62,973
θ_{GATA}	41,499	39,356	47,646

Note: Table shows point estimates and lower and upper 95% confidence intervals for each parameter, which include the timing of population size change (T_{BOT}) and divergence (T_{DIV1} and T_{DIV2}), and mutation-scaled ancestral (θ_{ANC}, θ_{BOT} and $\theta_{POLA\text{-}AGUI}$) and contemporary ($\theta_{POLA}$, θ_{AGUI} and θ_{GATA}) effective population sizes. Estimates of time are given in units of generations (or years, with 1 generation per year). Note that contemporary effective population size for the population POLA (θ_{POLA}) was calculated from its levels of nucleotide diversity (π) and fixed in FASTSIMCOAL2 analyses to enable the estimation of all other demographic parameters (see Section 2.6 for further details).

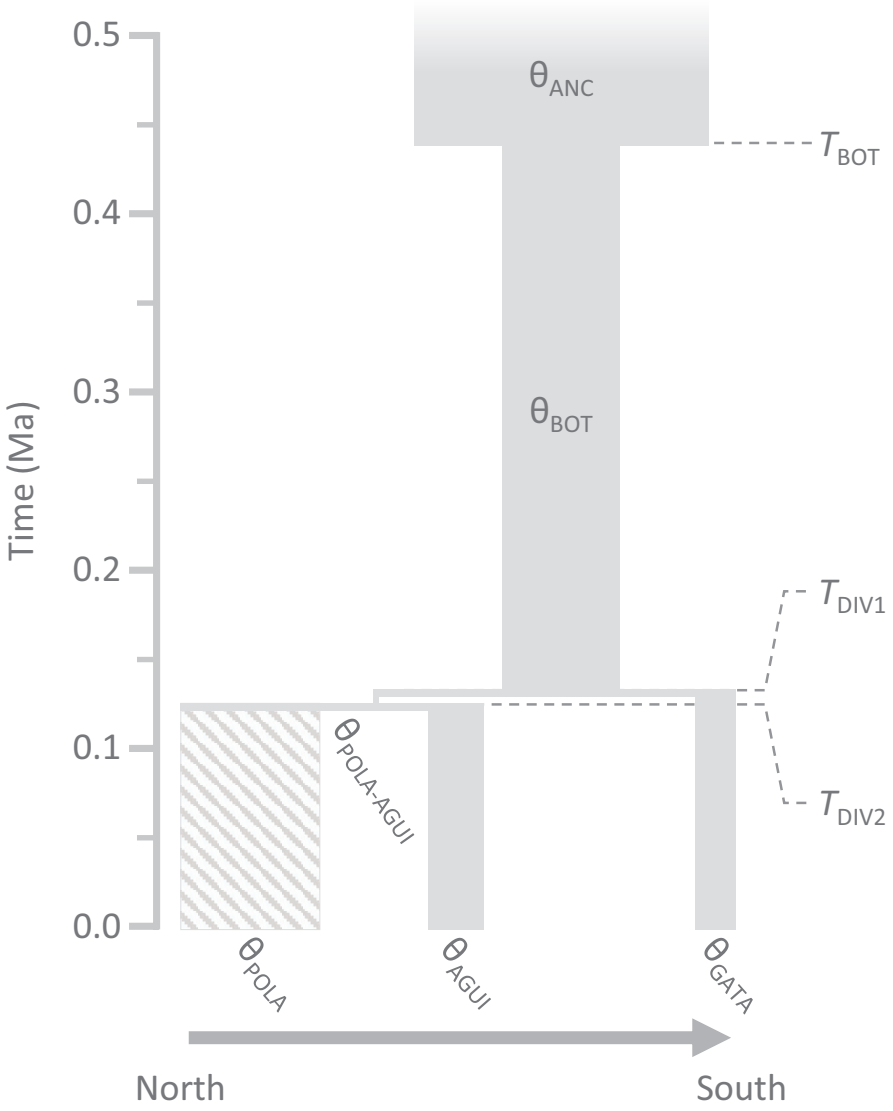

FIGURE 3 Schematic of the demographic model used in FASTSIMCOAL2 analyses to estimate the timing of colonization (i.e., hypothetically coinciding with a demographic bottleneck resulted from a founder event) of southeastern Iberia and in situ geographical diversification of *Dericorys carthagonovae*. Parameters include the timing of population size change (T_{BOT}) and divergence (T_{DIV1} and T_{DIV2}), and mutation-scaled ancestral (θ_{ANC}, θ_{BOT} and $\theta_{POLA\text{-}AGUI}$) and contemporary ($\theta_{POLA}$, θ_{AGUI} and θ_{GATA}) effective population sizes. Point estimates yielded by FASTSIMCOAL2 were used to scale the different time events (T) (left axis) and effective population sizes (θ, proportional to box width). Contemporary effective population size for the population POLA (θ_{POLA}, hatched box) was calculated from its levels of nucleotide diversity (π) and fixed in FASTSIMCOAL2 analyses to enable the estimation of all other demographic parameters (see Section 2.6 for further details). Demographic parameter values and confidence intervals are detailed in Table 2 and population codes are described in Table 1

$p < 0.001$; Hd: $t = 12.58$, $p < 0.001$; θ: $t = -17.96$, $p < 0.001$; Table 1; Figure 4).

3.7 | Environmental niche modelling

A threshold (*T*) feature class and a regularization multiplier of 2 minimized AICc across the set of tested models. After removing highly correlated variables ($r > 0.9$) and those with a zero percent contribution, the model retained seven bioclimatic variables (sorted by percent contribution, BIO12: 37.4%; BIO3: 34.5%; BIO15: 9.1%; BIO2: 9.0%; BIO6: 6.6%; BIO5: 3.2%; BIO8: 0.1%). Projections of the ENM to bioclimatic conditions from the LGM to present at 100-year intervals revealed that the extent of suitable areas, as identified using the maximum training sensitivity plus specificity threshold for species presence (Liu et al., 2005), sharply increased from the LGM to the onset of the Holocene (c. 12 ka), reached a maximum during the Holocene Climate Optimum (c. 9000 to 5000 years ago), and gradually declined since then (Figure 5). In the same line, environmentally suitable areas for the species were considerably fragmented during the LGM and these became much more connected along the Mediterranean coast of North Africa during the Holocene (Figure 5).

4 | DISCUSSION

Our results support the Pleistocene connectivity between northern African and southern European arid habitats and the strong genetic cohesiveness of thermophilous terrestrial faunas shared between the two continents (Husemann et al., 2014; e.g., Graciá, Giménez, et al., 2013; Habel et al., 2010; Noguerales et al., 2021). Divergence time estimates indicate that all trans-Mediterranean populations of *D. millierei* diverged during the Quaternary (<1.6 Ma) and phylogenomic and demographic analyses place the colonization of southeastern Iberia in the mid- to late Pleistocene (<0.5 Ma), supporting a transmarine migration event that might have taken place coinciding with sea-level lowering during glacial maxima (Graciá, Giménez, et al., 2013; Noguerales et al., 2021). Although these grasshoppers are good flyers and have a high intrinsic dispersal capacity, the

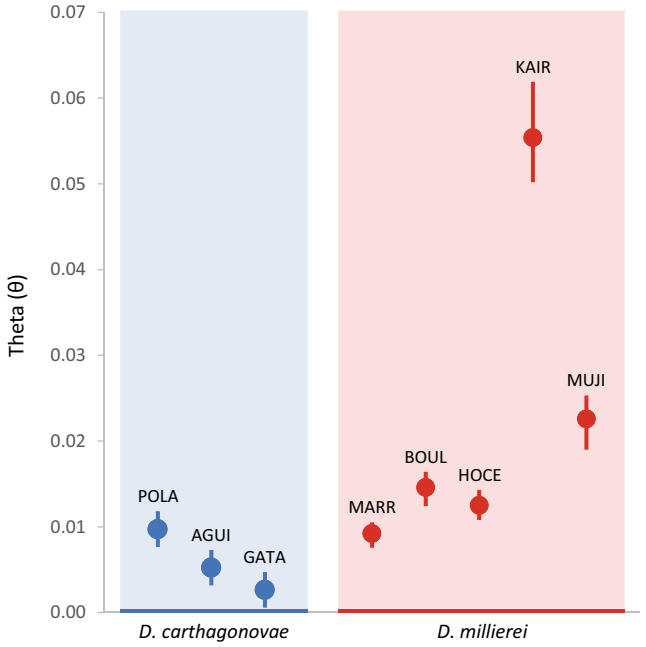

FIGURE 4 Estimates of the population size parameter (θ) (median ± 95% high posterior density intervals) inferred by SNAPP for the analysed populations of *Dericorys carthagonovae* and *D. millierei* across the Mediterranean region. Population codes as described in Table 1

marked genetic structure of their contemporary populations suggests that strong dependency on severely fragmented habitats has resulted in ancient disruptions of gene flow even among geographically close populations (Figure 1).

4.1 | Pleistocene dispersal and fragmentation

Our phylogenomic and dating analyses supported a Pleistocene divergence (<1.6 Ma) of all populations of *D. millierei*, indicating that the trans-Mediterranean distribution and marked genetic structure of contemporary populations of the species have been most probably shaped by pulses of population expansion-fragmentation linked to the high-amplitude climatic oscillations of the late Quaternary (Hewitt, 2004; Figure 5). This adds to the accumulating phylogeographic evidence supporting dispersal across North Africa at different time periods (e.g., Beddek et al., 2018; Escudero et al., 2010; Noguerales et al., 2021; Pérez-Collazos et al., 2009; Veríssimo et al., 2016), which indicates that this region has served as an important migration corridor for numerous terrestrial organisms and played a major role on faunal and floral exchanges between Asia, Africa and Europe (Husemann et al., 2014; Sanmartín, 2003). The main east-west split separating Moroccan from Tunisian populations is also congruent with findings from numerous previous studies in which the Moulouya River valley (Algeria-Morocco border) and the Kabylia region (central Algeria) have been identified as the main phylogeographic breaks across numerous organismal groups (e.g., land snails: Guiller & Madec, 2010; reptiles and amphibians: Beddek et al., 2018; plants: Sánchez-Gómez et al., 2013; Taib et al., 2020). Formal testing of concordance in divergence times across co-distributed taxa would help to distinguish among alternative biogeographical hypotheses and understand whether spatially similar phylogeographic structures correspond to contrasting evolutionary processes or to analogous responses to the past geological and/or climatic dynamics of the region (e.g., Papadopoulou & Knowles, 2015; Wan et al., 2021). The limited realized dispersal of *D. millierei*, as evidenced by the pronounced genetic structure of its populations, points to range fragmentation, rather than long-distance dispersal, as the most likely explanation for the current distribution gap of the species in Egypt (Figure 1; Cigliano et al., 2021). Accordingly, our palaeodistribution reconstructions at fine temporal resolution supported the presence of corridors of suitable habitats across the Mediterranean coast of Africa that connected the central Maghreb region and the Middle East during the warmer stages of the Pleistocene (i.e., the Holocene Climate Optimum; Figure 5d). This distribution gap in northeastern Africa is analogous to that reported for two other arid-dwelling taxa with trans-Mediterranean disjunct distributions of Pleistocene origin: the saltmarsh grasshopper (*Mioscirtus wagneri*; Noguerales et al., 2021) and the spur-thighed tortoise (*Testudo graeca*; Fritz et al., 2009). Collectively, these results suggest that the contraction of suitable habitats in northeastern Africa is the most parsimonious explanation for the contemporary disjunct distributions observed in some thermophilous organisms that probably presented wider distributions across the Mediterranean region during the warmest stages of the Pleistocene (Noguerales et al., 2021; Ribera & Blasco-Zumeta, 1998).

4.2 | Transmarine colonization of southeastern Iberia

Our phylogenomic analyses revealed that all populations of the Iberian *D. carthagonovae* are monophyletic and embedded within the Maghrebian-Levantine *D. millierei*, which is a paraphyletic taxon (Figure 2). This finding is in agreement with previous studies showing that southern European lineages of numerous thermophilous taxa are nested within North African clades (reviewed in Husemann et al., 2014). Estimates of divergence time indicate that the Iberian Peninsula was colonized from the Maghreb region during the Pleistocene (<0.5 Ma), supporting a post-Messinian transmarine dispersal event. The split of the different lineages of both *D. millierei* and *D. carthagonovae* probably took place during the coldest stages of the Pleistocene (i.e., glacial periods), when sea levels were below the current shoreline (Figure 2) and populations became highly fragmented according to palaeodistribution modelling (Figure 5f). Remarkably, phylogenomic and demographic analyses suggest that southeastern Iberia was colonized from the Maghreb region coinciding with the severe Mindel glaciation (c. 440 ka; Figures 2 and 3), a period that has been estimated to present the lowest sea level of the entire Pleistocene (−123 m; Figure S7; Miller et al., 2011). During this time, overseas distances between northern African and

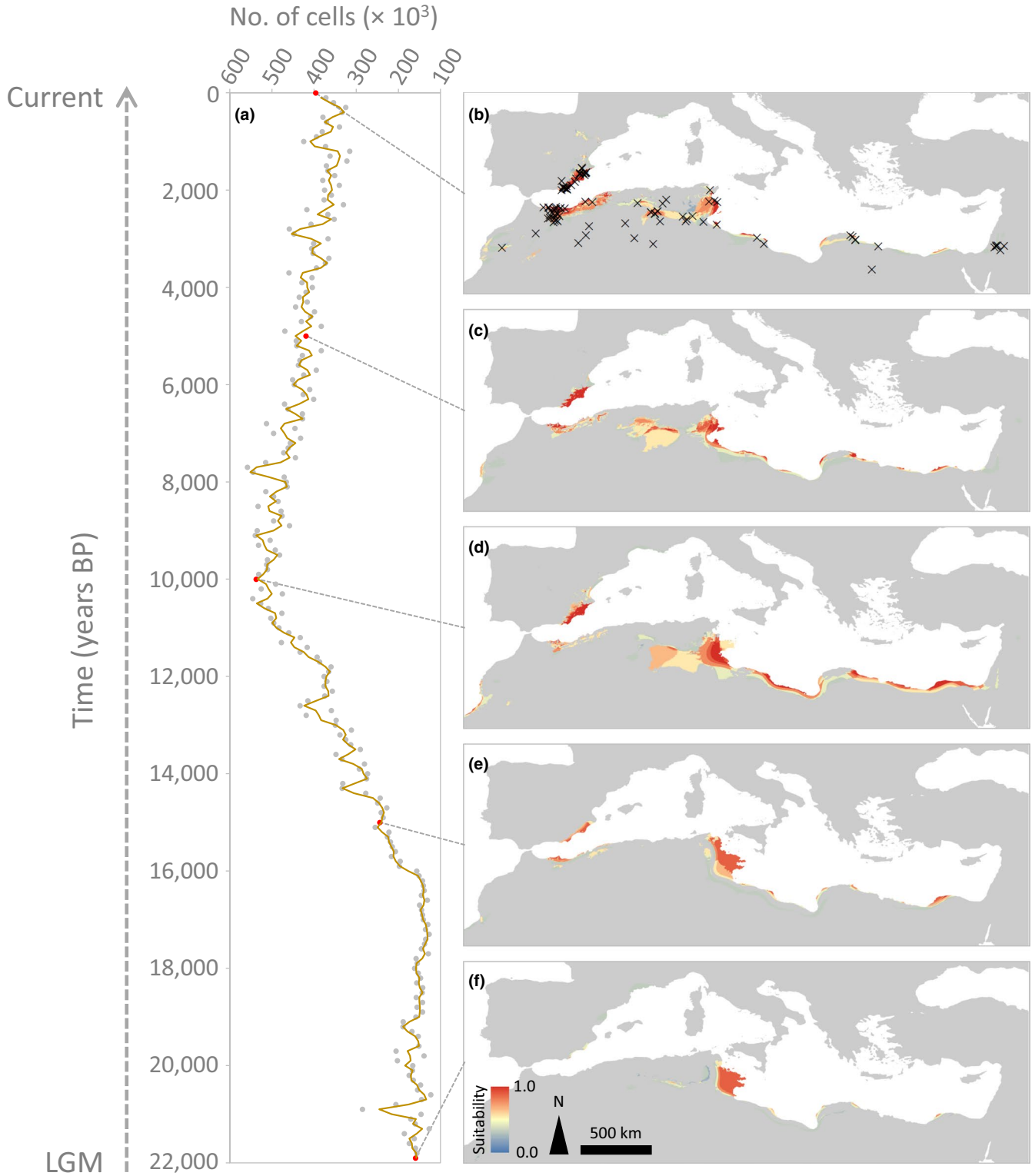

FIGURE 5 Extent of climatically suitable habitats for *Dericorys carthagonovae* and *D. millierei* as inferred from projections of the environmental niche model (ENM) to bioclimatic conditions during the last 22,000 years (i.e., from 1990 CE to the last glacial maximum, LGM) at 100-year time intervals. (a) The availability of suitable habitats at each time interval was calculated as the number of cells where the probability of presence of the species is higher than the maximum training sensitivity plus specificity (MTSS) logistic threshold. (b–f) Maps show the distribution of climatically suitable habitats for the species across the Mediterranean region at five temporal snapshots (red dots in panel a), including (b) the present (0 ka; crosses show occurrence points used for ENM), (d) Holocene Climate Optimum (c. 10 ka) and (f) LGM (c. 22 ka). Maps in EPSG:4326 (WGS84) projection

southern European landmasses were probably the shortest since the Messinian Salinity Crisis and lower sea levels might have resulted in the emergence of stepping-stone islands (e.g., shoals) and increased the chance of successful passive dispersal by rafting (Houle, 1998; Husemann et al., 2014). It must be noted, however, that estimates of divergence time must be interpreted with extreme caution considering uncertainty around genomic mutation rates and limited sample sizes for demographic analyses (Table 1). Lack of samples from Algeria, which could be the actual source populations from which southeastern Iberia was colonized (e.g., Graciá, Giménez, et al., 2013), also add considerable spatial and temporal uncertainty in stem age estimates (García-Verdugo et al., 2019). In this line, it has been recently suggested that colonization times most likely lie within the time period between stem (i.e., the split between North African and southeastern Iberian lineages) and crown (i.e., time of the most recent common ancestor of southeastern Iberian populations) age estimates, which would place the arrival of the species to the Iberian Peninsula more recently (<0.3 Ma; Figures 2 and 3; see García-Verdugo et al., 2019).

Phylogenomic reconstructions, palaeodistribution modelling and spatial patterns of genetic diversity provided some clues about the potential areas of origin and arrival of southeastern Iberia populations. Strikingly, *D. carthagonovae* shared a sister relationship with populations of *D. millierei* from Tunisia (KAIR), which are separated from the nearest Iberian populations by >1000 km (Figure 1). This geographical distance is considerably much longer than that separating *D. carthagonovae* from the nearest genotyped population of *D. millierei* from northern Morocco (<200 km; ALHU; Figure 1). Tunisia was identified by palaeodistribution modelling as the most suitable area for the species through the entire Pleistocene and also as the largest and one of the few suitable spots for the species during the LGM (Figure 5f), which might explain its extraordinarily high levels of genetic diversity in comparison with the rest of the populations and support this region as a candidate source population for the colonization of the Iberian Peninsula (Figure 2). Another non-mutually exclusive possibility to explain the high genetic diversity of Tunisian populations is that this region is a melting pot of western and eastern lineages (e.g., Dinis et al., 2019), which could also explain the uncertain phylogenetic position of Jordanian populations (Figure 1; Figure S5). Given that propagule numbers in transmarine dispersal events are expected to be extraordinarily low, a considerable loss of genetic diversity during the colonization of the Iberian Peninsula is, therefore, the most likely scenario (i.e., founder effect; Carson & Templeton, 1984). In this line, genetic diversity of Iberian populations is pretty similar to that inferred for populations from Morocco, but much lower than those obtained for the putative source populations in Tunisia (Figure 4).

Although sampling gaps in North Africa (Algeria and Libya; Figure 1) does not allow us to identify the precise location of founder populations, our results are in line with a few previous studies showing that thermophilous terrestrial organisms narrowly distributed in semiarid areas of southeastern Iberia present a higher genetic affinity with central-eastern Maghreb (Algeria and Tunisia) lineages than with western Maghrebian (Morocco) populations located at shorter geographical and overseas distances. For instance, the spur-thighed tortoise (*Testudo graeca*) likely colonized southeastern Iberia from western Algeria after the last glacial period (Graciá, Giménez, et al., 2013) and relict populations of the Barbary thuja (*Tetraclinis articulata*) in southeastern Iberia genetically cluster together with Maltese and Tunisian populations rather than with the geographically closer populations from Algeria and Morocco (Sánchez-Gómez et al., 2013). In the same line, southern European populations of the viperine water snake (*Natrix maura*) are more closely related with Algerian and Tunisian populations than with Moroccan populations (Beddek et al., 2018). The fact that some of these species were utilized by humans in historical times (e.g., *Testudo graeca*: direct human consumption; *Tetraclinis articulata*: timber) has led to suggest the possibility of human-mediated dispersal, although this hypothesis was not formally tested (Sánchez-Gómez et al., 2013) or remained unresolved (Graciá, Giménez, et al., 2013). Our genomic-based age estimates confirm a post-Messinian colonization of the Iberian Peninsula by the ancestor of *D. carthagonovae* that largely predates the possibility of human-mediated transportation, supporting the hypothesis of transmarine natural dispersal (Figure 2). Importantly, these results indicate that Pleistocene faunal exchanges between southern Europe and northern Africa did not exclusively take place across the strait of Gibraltar and the Sicilian Channel and suggest that overseas dispersal of terrestrial organisms between the two continents might be much more common than previously thought (Delicado et al., 2014; Husemann et al., 2014; Stöck et al., 2008).

The north to south decline of genetic diversity in populations of *D. carthagonovae* (Figures 3 and 4; Table 1) suggests that the ancestral founder populations might have arrived in the northernmost portion of the current distribution of the species in the Iberian Peninsula followed by serial founder effects and loss of genetic diversity during southward range expansions (see also Graciá, Botella, et al., 2013). Fine-scale population sampling in combination with detailed landscape genetic and demographic analyses might help to determine whether the observed cline of genetic diversity reflects the expansion history (Graciá, Botella, et al., 2013) or if, rather, it is a consequence of local demographic dynamics linked to availability of suitable habitats and more contemporary patterns of genetic connectivity among remnant population of the species (González-Serna et al., 2019). Anyway, our dating analyses clearly indicate that the genetic divergence of the studied populations (>120 ka) largely predate the timing of extensive anthropogenic impacts in the region, supporting that contemporary genetic fragmentation is not a consequence of habitat destruction resulted from recent human activities (González-Serna et al., 2019; Zellmer & Knowles, 2009). In line with studies on other halophilic species (Ortego et al., 2010, 2015), strong genetic structure and lack of genetic exchange between nearby populations emphasize the limited realized dispersal of the species and the low chance that extirpated populations are re-colonized by natural dispersal (Hochkirch et al., 2016).

4.3 | Taxonomic and conservation implications

Genealogical and divergence time inferences revealed that *D. carthagonovae* is nested within *D. millierei* and indicate that its ancestor arrived to the Iberian Peninsula much later (< 0.5 Ma) than the estimated divergences among main lineages of *D. millierei* (>1 Ma). This suggests that *D. carthagonovae*, originally described by Bolívar (1897) as a "variety" of *D. millierei* and later upgraded to full species status by Kirby (1910) without any justification or re-description, must be synonymized with *D. millierei* (for a list of synonyms, see Cigliano et al., 2021). The conservation status of Iberian populations of the species should be re-evaluated but always taking into account its high singularity (i.e., it is the only representative of the genus in Europe) and the intrinsic value of occupied habitats, which have experienced a dramatic destruction in the last decades due to the extensive agricultural and urban development of the region (Hochkirch et al., 2016; Verdú et al., 2011; see also Peñas et al., 2011).

5 | CONCLUSIONS

This study illustrates the potential of integrating genomic data, eustatic sea-level reconstructions, and palaeodistribution modelling at fine temporal resolution to shed light on the processes underlying the distribution of thermophilous and arid-dwelling faunas shared between southern Europe and arid and desertic regions from North Africa. Our analyses revealed a post-Messinian geographical diversification of the crested grasshopper, supporting Pleistocene range expansion and overseas dispersal as the most parsimonious explanation for the current trans-Mediterranean distribution of *D. millierei* and the colonization of the Iberian Peninsula, respectively. Collectively, these findings highlight the high relevance of North Africa as a source of thermophilous European faunas and support the strong genetic affinities between the two continents despite the potential barrier effect of the Mediterranean Sea (Beddek et al., 2018; Husemann et al., 2014; Rodríguez-Sánchez et al., 2008). More detailed genetic sampling could help to define with more precision the colonization history of the Iberian Peninsula (e.g., Beddek et al., 2018) and experimental crossing attempts between Iberian and Maghrebian populations would allow to confirm the reproductive cohesiveness of their respective populations (Coyne & Orr, 1989; Saldamando et al., 2005). Future genomic studies focused on other co-distributed relict taxa from the semideserts of southeastern Iberia (e.g., Le Driant & Carlon, 2020; Pascual & Aguirre, 1996) would allow to test whether their colonization was the result of concerted (or idiosyncratic) responses to Pleistocene climatic/eustatic fluctuations, which might ultimately help to reach more generalizable conclusions about the processes underlying the biogeographic connections between African and southern European arid-dwelling biotas (Oaks et al., 2013; Papadopoulou & Knowles, 2015).

ACKNOWLEDGEMENTS

We wish to thank to Anna Papadopoulou for her valuable advice in data analyses, José Miguel Aparicio and Nabil Amor for their help during sampling, Anja Danielczak and Axel Hochkirch for providing us a specimen of *Dericorys minutus*, Sergio Pereira (The Centre for Applied Genomics) for Illumina sequencing, and three anonymous referees for their constructive and valuable comments on an earlier version of the manuscript. Francisco Rodríguez kindly provided us with pictures of *Dericorys carthagonovae*. We also thank Centro de Supercomputación de Galicia (CESGA) and Doñana's Singular Scientific-Technical Infrastructure (ICTS-RBD) for access to computer resources. Permits for collecting the red-listed *D. carthagonovae* and sampling in protected areas were granted by Region de Murcia (AUF/2016/0064), Junta de Andalucía (SGYBV/AF), Generalitat Valenciana (211/2014-VS), and Gobierno de Canarias (AFF168/13; 2020/18061). No other permits were required to conduct this study. Research was funded by the Spanish Ministry of Economy, Industry and Competitiveness and European Social Fund (grant numbers: CGL2011-25053, CGL2014-54671-P, CGL2016-80742-R, and CGL2017-83433-P).

CONFLICT OF INTEREST

The authors have no conflicts of interest to declare.

DATA AVAILABILITY STATEMENT

Raw Illumina reads have been deposited at the NCBI Sequence Read Archive (SRA) under BioProject PRJNA732001. Input files for all analyses are available for download on Figshare (https://doi.org/10.6084/m9.figshare.14706057).

ORCID

Joaquín Ortego https://orcid.org/0000-0003-2709-429X
María José González-Serna https://orcid.org/0000-0001-8688-7623
Víctor Noguerales https://orcid.org/0000-0003-3185-778X
Pedro J. Cordero https://orcid.org/0000-0002-1371-8009

REFERENCES

Barrientos, R., Kvist, L., Barbosa, A., Valera, F., López-Iborra, G. M., & Moreno, E. (2009). Colonization patterns and genetic structure of peripheral populations of the trumpeter finch (*Bucanetes githagineus*) from Northwest Africa, the Canary Islands and the Iberian Peninsula. *Journal of Biogeography*, *36*(2), 210–219.

Beddek, M., Zenboudji-Beddek, S., Geniez, P., Fathalla, R., Sourouille, P., Arnal, V., Dellaoui, B., Koudache, F., Telailia, S., Peyre, O., & Crochet, P.-A. (2018). Comparative phylogeography of amphibians and reptiles in Algeria suggests common causes for the east-west phylogeographic breaks in the Maghreb. *PLoS ONE*, *13*(8), e0201218. https://doi.org/10.1371/journal.pone.0201218

Bialik, O. M., Frank, M., Betzler, C., Zammit, R., & Waldmann, N. D. (2019). Two-step closure of the Miocene Indian Ocean Gateway to the Mediterranean. *Scientific Reports*, *9*, 8842. https://doi.org/10.1038/s41598-019-45308-7

Bolívar, I. (1897). Insectos recogidos en Cartagena por D. José Sánchez Gómez. *Actas de la Sociedad Española de Historia Natural*, *26*, 166–174.

Bryant, D., Bouckaert, R., Felsenstein, J., Rosenberg, N. A., & RoyChoudhury, A. (2012). Inferring species trees directly from biallelic genetic markers: Bypassing gene trees in a full coalescent analysis. *Molecular Biology and Evolution*, *29*(8), 1917–1932. https://doi.org/10.1093/molbev/mss086

Cabello, J., Alcaraz-Segura, D., Gómez-Mercado, F., Mota, J. F., Navarro, J., Peñas, J., & Giménez, E. (2003). Habitat, occurrence and

conservation of Saharo-Arabian-Turanian element *Forsskaolea tenacissima* L. in the Iberian Peninsula. *Journal of Arid Environments*, *53*(4), 491–500. https://doi.org/10.1006/jare.2002.1062

Carson, H. L., & Templeton, A. R. (1984). Genetic revolutions in relation to speciation phenomena: The founding of new populations. *Annual Review of Ecology and Systematics*, *15*, 97–131. https://doi.org/10.1146/annurev.es.15.110184.000525

Catchen, J. M., Amores, A., Hohenlohe, P., Cresko, W., & Postlethwait, J. H. (2011). STACKS: Building and genotyping loci *de novo* from short-read sequences. *G3-Genes Genomes Genetics*, *1*(3), 171–182. https://doi.org/10.1534/g3.111.000240

Catchen, J., Hohenlohe, P. A., Bassham, S., Amores, A., & Cresko, W. A. (2013). STACKS: An analysis tool set for population genomics. *Molecular Ecology*, *22*(11), 3124–3140. https://doi.org/10.1111/mec.12354

Chifman, J., & Kubatko, L. (2014). Quartet inference from SNP data under the coalescent model. *Bioinformatics*, *30*(23), 3317–3324. https://doi.org/10.1093/bioinformatics/btu530

Cigliano, M. M., Braun, H., Eades, D. C., & Otte, D. (2021). *Orthoptera species file (OSF)*. http://orthoptera.speciesfile.org

Coyne, J. A., & Orr, H. A. (1989). Patterns of speciation in *Drosophila*. *Evolution*, *43*(2), 362–381. https://doi.org/10.2307/2409213

Delicado, D., Machordom, A., & Ramos, M. A. (2014). Vicariant versus dispersal processes in the settlement of *Pseudamnicola* (Caenogastropoda, Hydrobiidae) in the Mediterranean Balearic Islands. *Zoological Journal of the Linnean Society*, *171*(1), 38–71. https://doi.org/10.1111/zoj12124

Dinis, M., Merabet, K., Martínez-Freiría, F., Steinfartz, S., Vences, M., Burgon, J. D., Elmer, K. R., Donaire, D., Hinckley, A., Fahd, S., Joger, U., Fawzi, A., Slimani, T., & Velo-Antón, G. (2019). Allopatric diversification and evolutionary melting pot in a North African Palearctic relict: The biogeographic history of *Salamandra algira*. *Molecular Phylogenetics and Evolution*, *130*, 81–91. https://doi.org/10.1016/j.ympev.2018.10.018

Earl, D. A., & vonHoldt, B. M. (2012). STRUCTURE HARVESTER: A website and program for visualizing STRUCTURE output and implementing the Evanno method. *Conservation Genetics Resources*, *4*(2), 359–361. https://doi.org/10.1007/s12686-011-9548-7

Eaton, D. A. R. (2014). PYRAD: Assembly of *de novo* RADseq loci for phylogenetic analyses. *Bioinformatics*, *30*(13), 1844–1849. https://doi.org/10.1093/bioinformatics/btu121

Escudero, M., Vargas, P., Arens, P., Ouborg, N. J., & Luceño, M. (2010). The east-west-north colonization history of the Mediterranean and Europe by the coastal plant *Carex extensa* (Cyperaceae). *Molecular Ecology*, *19*(2), 352–370. https://doi.org/10.1111/j.1365-294X.2009.04449.x

Evanno, G., Regnaut, S., & Goudet, J. (2005). Detecting the number of clusters of individuals using the software STRUCTURE: A simulation study. *Molecular Ecology*, *14*(8), 2611–2620. https://doi.org/10.1111/j.1365-294X.2005.02553.x

Excoffier, L., Dupanloup, I., Huerta-Sánchez, E., Sousa, V. C., & Foll, M. (2013). Robust demographic inference from genomic and SNP data. *PLoS Genetics*, *9*(10), e1003905. https://doi.org/10.1371/journal.pgen.1003905

Faille, A., Andújar, C., Fadrique, F., & Ribera, I. (2014). Late Miocene origin of an Ibero-Maghrebian clade of ground beetles with multiple colonizations of the subterranean environment. *Journal of Biogeography*, *41*(10), 1979–1990. https://doi.org/10.1111/jbi.12349

Flouri, T., Jiao, X. Y., Rannala, B., & Yang, Z. H. (2018). Species tree inference with BPP using genomic sequences and the multispecies coalescent. *Molecular Biology and Evolution*, *35*(10), 2585–2593. https://doi.org/10.1093/molbev/msy147

Fritz, U., Harris, D. J., Fahd, S., Rouag, R., Graciá Martínez, E., Giménez Casalduero, A., Široký, P., Kalboussi, M., Jdeidi, T. B., & Hundsdörfer, A. K. (2009). Mitochondrial phylogeography of *Testudo graeca* in the Western Mediterranean: Old complex divergence in North Africa and recent arrival in Europe. *Amphibia-Reptilia*, *30*(1), 63–80. https://doi.org/10.1163/156853809787392702

García-Verdugo, C., Caujape-Castells, J., & Sanmartín, I. (2019). Colonization time on island settings: Lessons from the Hawaiian and Canary Island floras. *Botanical Journal of the Linnean Society*, *191*(2), 155–163. https://doi.org/10.1093/botlinnean/boz044

González-Serna, M. J., Cordero, P. J., & Ortego, J. (2019). Spatiotemporally explicit demographic modelling supports a joint effect of historical barriers to dispersal and contemporary landscape composition on structuring genomic variation in a red-listed grasshopper. *Molecular Ecology*, *28*(9), 2155–2172. https://doi.org/10.1111/mec.15086

Graciá, E., Botella, F., Anadón, J. D., Edelaar, P., Harris, D. J., & Giménez, A. (2013). Surfing in tortoises? Empirical signs of genetic structuring owing to range expansion. *Biology Letters*, *9*(3), 20121091. https://doi.org/10.1098/rsbl.2012.1091

Graciá, E., Giménez, A., Anadon, J. D., Harris, D. J., Fritz, U., & Botella, F. (2013). The uncertainty of Late Pleistocene range expansions in the western Mediterranean: A case study of the colonization of southeastern Spain by the spur-thighed tortoise, *Testudo graeca*. *Journal of Biogeography*, *40*(2), 323–334. https://doi.org/10.1111/jbi.12012

Guiller, A., & Madec, L. (2010). Historical biogeography of the land snail *Cornu aspersum*: A new scenario inferred from haplotype distribution in the Western Mediterranean basin. *BMC Evolutionary Biology*, *10*, 18. https://doi.org/10.1186/1471-2148-10-18

Habel, J. C., Rodder, D., Stefano, S., Meyer, M., & Schmitt, T. (2010). Strong genetic cohesiveness between Italy and North Africa in four butterfly species. *Biological Journal of the Linnean Society*, *99*(4), 818–830. https://doi.org/10.1111/j.1095-8312.2010.01394.x

Hewitt, G. M. (2004). Genetic consequences of climatic oscillations in the Quaternary. *Philosophical Transactions of the Royal Society of London Series B-Biological Sciences*, *359*(1442), 183–195.

Hochkirch, A., Presa, J. J., García, M., Barranco Vega, P., Correas, J., Ferreira, S., Lemos, P., & Prunier, F. (2016). *Dericorys carthagonovae: The IUCN red list of threatened species 2016* (Publication no. e.T16084510A74251711). https://doi.org/10.2305/IUCN.UK.2016-3.RLTS.T16084510A74251711.en. https://www.iucnredlist.org/species/16084510/74251711

Houle, A. (1998). Floating islands: A mode of long-distance dispersal for small and medium-sized terrestrial vertebrates. *Diversity & Distributions*, *4*(5–6), 201–216.

Huang, J. P., Hill, J. G., Ortego, J., & Knowles, L. L. (2020). Paraphyletic species no more – Genomic data resolve a Pleistocene radiation and validate morphological species of the *Melanoplus scudderi* complex (Insecta: Orthoptera). *Systematic Entomology*, *45*(3), 594–605. https://doi.org/10.1111/syen.12415

Husemann, M., Schmitt, T., Zachos, F. E., Ulrich, W., & Habel, J. C. (2014). Palaearctic biogeography revisited: Evidence for the existence of a North African refugium for Western Palaearctic biota. *Journal of Biogeography*, *41*(1), 81–94. https://doi.org/10.1111/jbi.12180

Jakobsson, M., & Rosenberg, N. A. (2007). CLUMPP: A cluster matching and permutation program for dealing with label switching and multimodality in analysis of population structure. *Bioinformatics*, *23*(14), 1801–1806. https://doi.org/10.1093/bioinformatics/btm233

Jombart, T. (2008). 'adegenet': A R package for the multivariate analysis of genetic markers. *Bioinformatics*, *24*(11), 1403–1405. https://doi.org/10.1093/bioinformatics/btn129

Kajtoch, L., Cieslak, E., Varga, Z., Paul, W., Mazur, M. A., Sramko, G., & Kubisz, D. (2016). Phylogeographic patterns of steppe species in Eastern Central Europe: A review and the implications for conservation. *Biodiversity and Conservation*, *25*(12), 2309–2339. https://doi.org/10.1007/s10531-016-1065-2

Karger, D. N., Conrad, O., Böhner, J., Kawohl, T., Kreft, H., Soria-Auza, R. W., Zimmermann, N. E., Linder, H. P., & Kessler, M. (2017). Climatologies at high resolution for the earth's land surface areas. *Scientific Data*, *4*, 170122. https://doi.org/10.1038/sdata.2017.122

Karger, D. N., Conrad, O., Bohner, J., Kawohl, T., Kreft, H., Soria-Auza, R. W., Zimmermann, N. E., Linder, H. P., & Kessler, M. (2017). Data from: Climatologies at high resolution for the earth's land surface areas. *Dryad Digital Repository*. https://doi.org/10.5061/dryad.kd1d4

Keightley, P. D., Ness, R. W., Halligan, D. L., & Haddrill, P. R. (2014). Estimation of the spontaneous mutation rate per nucleotide site in a *Drosophila melanogaster* full-sib family. *Genetics*, *196*(1), 313–320. https://doi.org/10.1534/genetics.113.158758

Kirby, W. F. (1910). *A Synonymic Catalogue of Orthoptera. Vol. 3. Orthoptera saltatoria Part II (Locustidae vel Acridiidae)*. London British Museum.

Kirschner, P., Záveská, E., Gamisch, A., Hilpold, A., Trucchi, E., Paun, O., Sanmartín, I., Schlick-Steiner, B. C., Frajman, B., Arthofer, W., Steiner, F. M., & Schönswetter, P.; … Consortium, S. (2020). Long-term isolation of European steppe outposts boosts the biome's conservation value. *Nature Communications*, *11*(1). 1968. https://doi.org/10.1038/s41467-020-15620-2

Le Driant, F., & Carlon, L. (2020). The Saharo-Arabian *Gymnocarpos sclerocephalus* (Caryophyllaceae) new to Europe in the semideserts of Almeria, Spain. *Willdenowia*, *50*(2), 187–194. https://doi.org/10.3372/wi.50.50204

Liu, C. R., Berry, P. M., Dawson, T. P., & Pearson, R. G. (2005). Selecting thresholds of occurrence in the prediction of species distributions. *Ecography*, *28*(3), 385–393. https://doi.org/10.1111/j.0906-7590.2005.03957.x

Liu, Z., Otto-Bliesner, B. L., He, F., Brady, E. C., Tomas, R., Clark, P. U., Carlson, A. E., Lynch-Stieglitz, J., Curry, W., Brook, E., Erickson, D., Jacob, R., Kutzbach, J., & Cheng, J. (2009). Transient simulation of last deglaciation with a new mechanism for bolling-allerod warming. *Science*, *325*(5938), 310–314. https://doi.org/10.1126/science.1171041

Manafzadeh, S., Salvo, G., & Conti, E. (2014). A tale of migrations from east to west: The Irano-Turanian floristic region as a source of Mediterranean xerophytes. *Journal of Biogeography*, *41*(2), 366–379. https://doi.org/10.1111/jbi.12185

Martínez-Solano, I., Gonçalves, H. A., Arntzen, J. W., & García-París, M. (2004). Phylogenetic relationships and biogeography of midwife toads (Discoglossidae: *Alytes*). *Journal of Biogeography*, *31*(4), 603–618. https://doi.org/10.1046/j.1365-2699.2003.01033.x

Meulenkamp, J. E., & Sissingh, W. (2003). Tertiary palaeogeography and tectonostratigraphic evolution of the Northern and Southern Peri-Tethys platforms and the intermediate domains of the African-Eurasian convergent plate boundary zone. *Palaeogeography Palaeoclimatology Palaeoecology*, *196*(1–2), 209–228. https://doi.org/10.1016/s0031-0182(03)00319-5

Miller, K. G., Mountain, G. S., Wright, J. D., & Browning, J. V. (2011). A 180-million-year record of sea level and ice volume variations from continental margin and deep-sea isotopic records. *Oceanography*, *24*(2), 40–53. https://doi.org/10.5670/oceanog.2011.26

Noguerales, V., Cordero, P. J., Knowles, L. L., & Ortego, J. (2021). Genomic insights into the origin of trans-Mediterranean disjunct distributions. *Journal of Biogeography*, *48*(2), 440–452. https://doi.org/10.1111/jbi.14011

Noguerales, V., Cordero, P. J., & Ortego, J. (2018). Integrating genomic and phenotypic data to evaluate alternative phylogenetic and species delimitation hypotheses in a recent evolutionary radiation of grasshoppers. *Molecular Ecology*, *27*(5), 1229–1244. https://doi.org/10.1111/mec.14504

Oaks, J. R., Sukumaran, J., Esselstyn, J. A., Linkem, C. W., Siler, C. D., Holder, M. T., & Brown, R. M. (2013). Evidence for climate-driven diversification? A caution for interpreting ABC inferences of simultaneous historical events. *Evolution*, *67*(4), 991–1010. https://doi.org/10.1111/j.1558-5646.2012.01840.x

Ortego, J., Aguirre, M. P., & Cordero, P. J. (2010). Population genetics of *Mioscirtus wagneri*, a grasshopper showing a highly fragmented distribution. *Molecular Ecology*, *19*(3), 472–483. https://doi.org/10.1111/j.1365-294X.2009.04512.x

Ortego, J., García-Navas, V., Noguerales, V., & Cordero, P. J. (2015). Discordant patterns of genetic and phenotypic differentiation in five grasshopper species codistributed across a microreserve network. *Molecular Ecology*, *24*(23), 5796–5812. https://doi.org/10.1111/mec.13426

Ortego, J., Gugger, P. F., & Sork, V. L. (2018). Genomic data reveal cryptic lineage diversification and introgression in Californian golden cup oaks (section *Protobalanus*). *New Phytologist*, *218*(2), 804–818. https://doi.org/10.1111/nph.14951

Papadopoulou, A., & Knowles, L. L. (2015). Species-specific responses to island connectivity cycles: Refined models for testing phylogeographic concordance across a Mediterranean Pleistocene Aggregate Island Complex. *Molecular Ecology*, *24*(16), 4252–4268. https://doi.org/10.1111/mec.13305

Pascual, F., & Aguirre, A. (1996). Description of *Xerohippus occidentalis* sp. n., a new Gomphocerinae (Orthoptera, Acrididae) from the southern of the Iberian Peninsula (Almeria, Spain), with remarks on the genus distribution. *Zoologica Baetica*, *7*, 91–102.

Peñas, J., Benito, B., Lorite, J., Ballesteros, M., Cañadas, E. M., & Martínez-Ortega, M. (2011). Habitat fragmentation in arid zones: A case study of *Linaria nigricans* under land use changes (SE Spain). *Environmental Management*, *48*(1), 168–176. https://doi.org/10.1007/s00267-011-9663-y

Pérez-Collazos, E., Sánchez-Gómez, P., Jiménez, J. F., & Catalán, P. (2009). The phylogeographical history of the Iberian steppe plant *Ferula loscosii* (Apiaceae): A test of the abundant-centre hypothesis. *Molecular Ecology*, *18*(5), 848–861. https://doi.org/10.1111/j.1365-294X.2008.04060.x

Peterson, B. K., Weber, J. N., Kay, E. H., Fisher, H. S., & Hoekstra, H. E. (2012). Double digest RADseq: An inexpensive method for *de novo* SNP discovery and genotyping in model and non-model species. *PLoS ONE*, *7*(5), e37135. https://doi.org/10.1371/journal.pone.0037135

Phillips, S. J., Anderson, R. P., & Schapire, R. E. (2006). Maximum entropy modeling of species geographic distributions. *Ecological Modelling*, *190*(3–4), 231–259. https://doi.org/10.1016/j.ecolmodel.2005.03.026

Phillips, S. J., & Dudik, M. (2008). Modeling of species distributions with MAXENT: New extensions and a comprehensive evaluation. *Ecography*, *31*(2), 161–175. https://doi.org/10.1111/j.0906-7590.2008.5203.x

Pickrell, J. K., & Pritchard, J. K. (2012). Inference of population splits and mixtures from genome-wide allele frequency data. *PLoS Genetics*, *8*(11), e1002967. https://doi.org/10.1371/journal.pgen.1002967

Pritchard, J. K., Stephens, M., & Donnelly, P. (2000). Inference of population structure using multilocus genotype data. *Genetics*, *155*(2), 945–959. https://doi.org/10.1093/genetics/155.2.945

R Core Team. (2021). *r: A language and environment for statistical computing*. R Foundation for Statistical Computing. https://www.R-project.org/

Rannala, B., & Yang, Z. H. (2003). Bayes estimation of species divergence times and ancestral population sizes using DNA sequences from multiple loci. *Genetics*, *164*(4), 1645–1656. https://doi.org/10.1093/genetics/164.4.1645

Ribera, I., & Blasco-Zumeta, J. (1998). Biogeographical links between steppe insects in the Monegros region (Aragon, NE Spain), the eastern Mediterranean, and central Asia. *Journal of Biogeography*, *25*(5), 969–986. https://doi.org/10.1046/j.1365-2699.1998.00226.x

Rodríguez-Sánchez, F., Pérez-Barrales, R., Ojeda, F., Vargas, P., & Arroyo, J. (2008). The Strait of Gibraltar as a melting pot for plant biodiversity. *Quaternary Science Reviews*, *27*(23–24), 2100–2117. https://doi.org/10.1016/j.quascirev.2008.08.006

Rosenberg, N. A. (2004). DISTRUCT: A program for the graphical display of population structure. *Molecular Ecology Notes*, *4*(1), 137–138. https://doi.org/10.1046/j.1471-8286.2003.00566.x

Rozas, J., Ferrer-Mata, A., Sánchez-DelBarrio, J. C., Guirao-Rico, S., Librado, P., Ramos-Onsins, S. E., & Sánchez-Gracia, A. (2017).

DNASP 6: DNA sequence polymorphism analysis of large data sets. *Molecular Biology and Evolution*, *34*(12), 3299–3302. https://doi.org/10.1093/molbev/msx248

Saldamando, C. I., Tatsuta, H., & Butlin, R. K. (2005). Hybrids between *Chorthippus brunneus* and *C. jacobsi* (Orthoptera: Acrididae) do not show endogenous postzygotic isolation. *Biological Journal of the Linnean Society*, *84*(2), 195–203. https://doi.org/10.1111/j.1095-8312.2005.000424.x

Sánchez-Gómez, P., Jiménez, J. F., Vera, J. B., Sánchez-Saorin, F. J., Martínez, J. F., & Buhagiar, J. (2013). Genetic structure of *Tetraclinis articulata*, an endangered conifer of the western Mediterranean basin. *Silva Fennica*, *47*(5), 1073. https://doi.org/10.14214/sf.1073

Sanmartín, I. (2003). Dispersal vs. vicariance in the Mediterranean: Historical biogeography of the Palearctic Pachydeminae (Coleoptera, Scarabaeoidea). *Journal of Biogeography*, *30*(12), 1883–1897.

Solís-Lemus, C., Bastide, P., & Ane, C. (2017). PHYLONETWORKS: A package for phylogenetic networks. *Molecular Biology and Evolution*, *34*(12), 3292–3298. https://doi.org/10.1093/molbev/msx235

Stöck, M., Sicilia, A., Belfiore, N. M., Buckley, D., Lo Brutto, S., Lo Valvo, M., & Arculeo, M. (2008). Post-Messinian evolutionary relationships across the Sicilian channel: Mitochondrial and nuclear markers link a new green toad from Sicily to African relatives. *BMC Evolutionary Biology*, *8*, 56. https://doi.org/10.1186/1471-2148-8-56

Taib, A., Morsli, A., Chojnacka, A., Walas, Ł., Sękiewicz, K., Boratyński, A., Romo, À., & Dering, M. (2020). Patterns of genetic diversity in North Africa: Moroccan-Algerian genetic split in *Juniperus thurifera* subsp. *africana*. *Scientific Reports*, *10*(1), 4810. https://doi.org/10.1038/s41598-020-61525-x

Takahashi, T., Nagata, N., & Sota, T. (2014). Application of RAD-based phylogenetics to complex relationships among variously related taxa in a species flock. *Molecular Phylogenetics and Evolution*, *80*, 137–144. https://doi.org/10.1016/j.ympev.2014.07.016

Tonzo, V., Papadopoulou, A., & Ortego, J. (2020). Genomic footprints of an old affair: Single nucleotide polymorphism data reveal historical hybridization and the subsequent evolution of reproductive barriers in two recently diverged grasshoppers with partly overlapping distributions. *Molecular Ecology*, *29*(12), 2254–2268. https://doi.org/10.1111/mec.15475

Verdú, J. R., Numa, C., & Galante, E. (2011). *Atlas y libro rojo de los invertebrados Amenazados de España (Especies Vulnerables)*. Dirección General de Medio Natural y Política Forestal, Ministerio de Medio Ambiente, Medio Rural y Marino.

Verissimo, J., Znari, M., Stuckas, H., Fritz, U., Pereira, P., Teixeira, J., Arculeo, M., Marrone, F., Sacco, F., Naimi, M., Kehlmaier, C., & Velo-Antón, G. (2016). Pleistocene diversification in Morocco and recent demographic expansion in the Mediterranean pond turtle *Mauremys leprosa*. *Biological Journal of the Linnean Society*, *119*(4), 943–959. https://doi.org/10.1111/bij.12849

Walsh, B. (2001). Estimating the time to the most recent common ancestor for the Y chromosome or mitochondrial DNA for a pair of individuals. *Genetics*, *158*(2), 897–912. https://doi.org/10.1093/genetics/158.2.897

Wan, T., Oaks, J. R., Jiang, X. L., Huang, H. T., & Knowles, L. L. (2021). Differences in Quaternary co-divergence reveals community-wide diversification in the mountains of southwest China varied among species. *Proceedings of the Royal Society B-Biological Sciences*, *288*(1942), 20202567. https://doi.org/10.1098/rspb.2020.2567

Yannic, G., Hagen, O., Leugger, F., Karger, D. N., & Pellissier, L. (2020). Harnessing paleo-environmental modeling and genetic data to predict intraspecific genetic structure. *Evolutionary Applications*, *13*(6), 1526–1542. https://doi.org/10.1111/eva.12986

Zellmer, A. J., & Knowles, L. L. (2009). Disentangling the effects of historic vs. contemporary landscape structure on population genetic divergence. *Molecular Ecology*, *18*(17), 3593–3602. https://doi.org/10.1111/j.1365-294X.2009.04305.x

BIOSKETCH

Joaquín Ortego is a researcher at Estación Biológica de Doñana (EBD-CSIC, Seville, Spain) broadly interested in evolutionary biogeography and the study of the processes underlying spatial patterns of genetic variation in different organism groups. More information about the laboratory and ongoing research projects can be found at https://www.ortegolab.com/.

Author contributions: JO designed the study and analyses. JO, VN and PJC collected the samples. MGS performed the lab work guided by JO. JO and MGS analysed the data. JO wrote the manuscript, with inputs from VN and PJC.

SUPPORTING INFORMATION

Additional supporting information may be found online in the Supporting Information section.

How to cite this article: Ortego, J., González-Serna, M. J., Noguerales, V., & Cordero, P. J. (2021). Genomic inferences in a thermophilous grasshopper provide insights into the biogeographic connections between northern African and southern European arid-dwelling faunas. *Journal of Biogeography*, 00, 1–15. https://doi.org/10.1111/jbi.14267